

Multivariate Conformal Prediction via Conformalized Gaussian Scoring

Sacha Braun¹, Eugène Berta¹, Michael I. Jordan^{1,2}, and Francis Bach¹

¹Sierra team, Inria Paris, France

{sacha.braun, eugene.bertha, francis.bach}@inria.fr

²Departments of EECS and Statistics, UC Berkeley, USA

jordan@cs.berkeley.edu

Abstract

While achieving exact conditional coverage in conformal prediction is unattainable without making strong, untestable regularity assumptions, the promise of conformal prediction hinges on finding approximations to conditional guarantees that are realizable in practice. A promising direction for obtaining conditional dependence for conformal sets—in particular capturing heteroskedasticity—is through estimating the conditional density $\mathbb{P}_{Y|X}$ and conformalizing its level sets. Previous work in this vein has focused on nonconformity scores based on the empirical cumulative distribution function (CDF). Such scores are, however, computationally costly, typically requiring expensive sampling methods. To avoid the need for sampling, we observe that the CDF-based score reduces to a Mahalanobis distance in the case of Gaussian scores, yielding a closed-form expression that can be directly conformalized. Moreover, the use of a Gaussian-based score opens the door to a number of extensions of the basic conformal method; in particular, we show how to construct conformal sets with missing output values, refine conformal sets as partial information about Y becomes available, and construct conformal sets on transformations of the output space. Finally, empirical results indicate that our approach produces conformal sets that more closely approximate conditional coverage in multivariate settings compared to alternative methods.

1 Introduction

Conformal prediction provides a powerful, model-agnostic framework for constructing predictive sets with guaranteed finite-sample marginal coverage (Vovk et al., 2005; Shafer and Vovk, 2008). Its flexibility makes it applicable to a wide range of predictive models, including black-box predictors. Achieving exact conditional coverage is provably impossible without additional assumptions (Vovk, 2012; Lei and Wasserman, 2014; Foygel Barber et al., 2021), and standard conformal methods, which typically construct the same predictive set around every point estimate, fail at even the core task of capturing heteroskedasticity. It remains an urgent agenda item for conformal prediction to improve empirical conditional coverage.

One reasonable path forward is to make use of quantile regression, which estimates quantiles of the conditional distribution, and therefore is adaptive to data heteroskedasticity (Romano et al., 2019; Angelopoulos and Bates, 2023). Another possibility is to attempt to estimate entire conditional densities

rather than focusing on specific quantiles. In principle, density estimation is not tied to a single coverage level, enabling more flexible and informative uncertainty quantification.

To date, work on density estimation in the conformal setting has focused on making minimal assumptions about the underlying distribution and fitting density functions via nonparametric or semi-parametric methods (Sampson and Chan, 2024; Dheur et al., 2025). This approach requires addressing the classical challenges of multi-modal density estimation, and additionally must face the issue of translating density estimates into interpretable point predictions or constructing conformal sets on top of an existing point predictor.

Our approach follows in the density estimation vein, but we take a different tack—we study simple, parametric density models. We will see that this approach is able to more closely approximate conditional coverage than existing methods and it enables several extensions of standard conformal prediction.

Our point of departure is a line of work initiated by Sadinle et al. (2019), who introduced likelihood-based non-conformity scores to produce conformal sets. Although this approach is adaptive to heteroskedasticity, unfortunately the resulting sets can be empty when the predicted conditional distribution of the output has a large variance. As a result, even if the model perfectly fits the true distribution of the data, conditional coverage is not achieved. To overcome this difficulty, Izbicki et al. (2022) suggested using a generalized cumulative distribution function (CDF) as a conformity score, yielding confidence intervals that are robust to the variance in the estimated density. When the estimated density $\hat{p}(Y | X)$, where X is a feature vector in \mathcal{X} and Y is the response vector in \mathcal{Y} , approaches the true conditional distribution $\mathbb{P}_{Y|X}$, this score achieves asymptotic conditional coverage. However, this score is not in closed form and requires estimating potentially high-dimensional integrals, which can be computationally intractable.

In this paper, we introduce *Gaussian-conformal prediction*, a framework that leverages a Gaussian model to learn feature-dependent uncertainty. We estimate the conditional density $\mathbb{P}_{Y|X}$ with $\mathcal{N}(f(X), \Sigma(X))$ where $f(X) \in \mathbb{R}^k$ and $\Sigma(X) \in \mathbb{R}^{k \times k}$ are feature-dependent functions targeting the mean vector and the covariance matrix, respectively. We use as a conformal score the local Mahalanobis distance induced by the feature-dependent covariance matrix of our Gaussian model $\sqrt{(f(X) - Y)^\top \Sigma^{-1}(X)(f(X) - Y)}$, and show that it is equivalent to the score proposed by Izbicki et al. (2022) under Gaussianity, which achieves asymptotic conditional coverage. Unlike other methods deriving from this theoretically grounded conformal score, we obtain closed-form formulas for our residuals and resulting conformal sets, leading to efficient inference and extension to higher dimensionality. We present a framework to fit the mean $f(\cdot)$ and covariance matrix $\Sigma(\cdot)$ by minimizing the cross-entropy loss induced by the associated Gaussian model (which is maximum likelihood estimation). The feature-dependent covariance matrix can be learned jointly with the mean or post hoc, on top of a fixed, user-specified, point predictor. This makes our method especially suited for constructing data-dependent conformal sets on top of existing, potentially black-box, point predictors. Moreover, the conformal sets can be computed efficiently by simply evaluating the point predictor $f(X)$ and the local covariance estimate $\Sigma(X)$.

In the univariate case, our method recovers the classical standardized residual score $|f(X) - Y|/\sigma(X)$, where $\sigma(X)$ is a learned, local uncertainty estimate. Fitting a local covariance matrix $\Sigma(X)$ and using the generalized standardized residual scores $\sqrt{(f(X) - Y)^\top \Sigma^{-1}(X)(f(X) - Y)}$ constitutes a natural extension to multivariate settings, resulting in elliptical predictive sets that better adapt

to the local uncertainty structure. Even when the data are not Gaussian, normalizing the residuals by their conditional covariance is expected to improve conditional coverage.

We emphasize that the size of the prediction set is not always the most appropriate criterion for comparing different conformal prediction strategies. Moreover, conformal prediction only ensures marginal coverage, and, as we show empirically, many existing methods tend to produce small prediction sets, even for the most uncertain instances, to the detriment of conditional coverage. This gives the user a misleading impression of controlling uncertainty, where the model deliberately fails to cover in certain regions of the input space (typically where the uncertainty is large), while compensating with over-coverage in other regions. In contrast, by conformalizing the level sets of the estimated density directly, our approach significantly improves empirical conditional coverage.

We also present a novel application of probabilistic inference to the problem of constructing multivariate conformal sets when there can be missing outputs in the dataset (i.e., some dimensions of the response vector are not observed). By leveraging quantiles of the fitted distribution, we can evaluate the quality of the predictive model regardless of the number of observed outputs. This setup enables the definition of a non-conformity score based on the quantile corresponding to the partially observed output. Using this score, we can infer a valid prediction set for the fully defined label, even when the training or calibration data are incomplete.

Another extension of conformal prediction enabled by our methods is to adjust conformal sets in the case of partially revealed outputs. For example, given a model predicting (Y^1, Y^2) , when the value Y^1 is revealed, our method allows us to adjust the confidence set for Y^2 . The more correlation between Y^1 and Y^2 , the more information we accrue and the more we can reduce the size of the adjusted confidence set. We also demonstrate how to construct a conformal set on a transformation of the output vector. For example, given a model predicting $(Y^1, Y^2, Y^3) \in \mathbb{R}^3$ the user might be interested in the transformation $(Y^1, Y^1 - Y^2)$. Taking into account the local covariance structure allows for more informative confidence sets on the combined variables. We motivate these two settings with illustrative examples in Sections 4 & 5 respectively.

Other frameworks have been developed to construct data-dependent conformal sets, but they have their limitations. Quantile regression fails to adjust to multivariate data, is not flexible in terms of coverage and cannot be built on top of existing predictors. For optimal transport strategies (Klein et al., 2025; Thurin et al., 2025), minimum volume conformal sets (Braun et al., 2025) and convex shape optimization (Tumu et al., 2024), we demonstrate empirically that the coverage obtained is less flexible than with our probabilistic approach. In particular, these frameworks either do not support the extensions that ours do or they produce overly conservative sets.

Summary of contributions. We develop a simple framework in which the conditional distribution of the output is estimated with a Gaussian model. We show that this yields conditionally robust conformal scores that can be computed in closed form. This allows for better empirical conditional coverage and also enables several extensions of traditional conformal prediction. Our method allows us to:

- Build confidence sets that are robust to heteroskedasticity in $\mathbb{P}_{Y|X}$ —from scratch or on top of an existing point predictor—by generalizing the popular standardized residuals to multivariate regression (Section 2).
- Construct conformal sets even when the available data has missing output values (Section 3).

- Refine the confidence set obtained when outputs are partially revealed (Section 4).
- Construct valid confidence sets on transformations of outputs (Section 5).

1.1 Related work

Conformal prediction for multivariate outputs presents the challenge of capturing dependencies between output dimensions, where simple hyperrectangle-based methods (Romano et al., 2019; Neeven and Smirnov, 2018) often fail. More flexible approaches attempt to fit complex shapes using multiple residuals. For example, Tumu et al. (2024) fit a convex set over all residuals, Johnstone and Cox (2021) use the empirical covariance matrix, and Thurin et al. (2025); Klein et al. (2025) apply optimal transport. However, these methods produce the same conformal set for every model output, thus lacking adaptivity to the input features. Some works introduce feature-adaptive methods (Messoudi et al., 2022), but they require computing the k-nearest neighbors for each feature vector X_i , which is computationally expensive both at conformalization and inference time.

Parametric methods that produce feature-dependent conformal sets (Braun et al., 2025) aim to overcome this challenge, but typically cannot guarantee conditional coverage. Density-based methods can construct adaptive conformal sets (Izbicki et al., 2022; Wang et al., 2023), yet the scoring functions become intractable in high dimensions. Plassier et al. (2025) introduced a sampling-based strategy to alleviate this burden, but the conformal sets obtained are random. Conditional variational autoencoders offer another path, but often involve directional quantile regression or cannot provide conformal sets on top of an existing point predictor (Feldman et al., 2023; English and Lippert, 2025).

Conformal prediction with missing values has received attention in the recent literature. Most existing work focuses on missingness in the input space (Zaffran et al., 2023, 2024; Kong et al., 2025). Some methods address noisy or corrupted outputs, but require strong assumptions on the data distribution or only handle label corruption (Zhou et al., 2025; Feldman et al., 2025).

To the best of our knowledge, conformal prediction under partial observability of outputs or output transformations has not been explored. The former resembles hierarchical output settings (Principato et al., 2024; Wieslander et al., 2020), while the latter could be approached by applying existing conformal methods directly to transformed outputs. However, parametric methods are generally not trained to accommodate such transformations. Among existing approaches, only those that estimate shapes using multiple residuals points naturally adjust to output transformations, though they are often suboptimal.

1.2 Background on conformal prediction with density estimation

This section focuses on *split conformal prediction*, a popular method known for its simplicity and computational efficiency in creating marginally valid prediction sets (Papadopoulos et al., 2002; Lei et al., 2018; Angelopoulos and Bates, 2023). Consider a dataset $\mathcal{D} = \{(X_i, Y_i)\}_{i=1}^n$, drawn from a distribution $\mathbb{P}_{X \times Y}$, where each $X_i \in \mathcal{X} \subseteq \mathbb{R}^d$ is a feature vector with d components, and each $Y_i \in \mathcal{Y} \subseteq \mathbb{R}^k$ is the response vector. The objective is to construct a prediction region $C_\alpha(X_{\text{test}})$ for a new test feature X_{test} such that it includes the true response Y_{test} with a probability of at least $1 - \alpha$.

To accomplish this, the dataset is divided into two parts: a *training dataset* \mathcal{D}_1 with n_1 samples, and a *calibration dataset* \mathcal{D}_2 with the remaining n_2 samples. Initially, a conditional probabilistic model $\hat{p}(Y|X)$ is fitted using the training dataset. The calibration dataset is then employed to assess the uncertainty of the model’s predictions by adjusting the prediction sets to ensure valid marginal

coverage. Specifically, conformal prediction aims to create a prediction region that meets the finite-sample guarantee:

$$\mathbb{P}_{X \times Y} (Y_{\text{test}} \in C_\alpha(X_{\text{test}})) \geq 1 - \alpha. \quad (1)$$

This probability accounts for the randomness in both the test point $(X_{\text{test}}, Y_{\text{test}})$ and the calibration set, assuming only that the data points are exchangeable without making further distributional assumptions.

A crucial element in achieving marginal coverage (1) is the selection of a *non-conformity score* function $S : \mathcal{X} \times \mathcal{Y} \rightarrow \mathbb{R}$, which quantifies how unusual an observed response Y is compared to the model’s prediction for a given feature vector X . After calculating the non-conformity scores for all calibration points, a threshold is determined by estimating the empirical $(1 - \alpha)$ -quantile of the distribution of these scores, adjusted with a *finite-sample correction*:

$$\hat{q}_\alpha = \text{Quantile} \left(\left[\frac{(1 - \alpha)(n_2 + 1)}{n_2} \right]; \frac{1}{n_2} \sum_{i=1}^{n_2} \delta_{S(X_i, Y_i)} \right). \quad (2)$$

This threshold defines the final prediction region for a test feature X_{test} as:

$$C_\alpha(X_{\text{test}}) = \{y \in \mathcal{Y} \mid S(X_{\text{test}}, y) \leq \hat{q}_\alpha\}. \quad (3)$$

By design, this region satisfies the finite-sample marginal coverage guarantee in (1), as the threshold is based on a rank statistic: the empirical quantile is chosen such that at least $\lceil (1 - \alpha)(n_2 + 1) \rceil$ calibration points have non-conformity scores below it. Given that the test point is exchangeable with the calibration points, its rank among them follows a uniform distribution, ensuring valid coverage.

Remark 1.1. Notice that marginal coverage (1) does not hold conditionally on the observed feature vector X_{test} but only marginally over the full distribution of X . This means that for a specific value X_{test} , the conformal set $C_\alpha(X_{\text{test}})$ will cover Y_{test} with an arbitrary probability, potentially smaller than $1 - \alpha$. The marginal coverage guarantee states that these local coverage levels average to $1 - \alpha$ over the distribution of feature vectors. By *conditional coverage* we refer to the stronger guarantee:

$$\mathbb{P}_{X \times Y} (Y_{\text{test}} \in C_\alpha(X_{\text{test}}) \mid X_{\text{test}}) \geq 1 - \alpha. \quad (4)$$

In a probabilistic prediction setting, where the model outputs an estimated probability distribution $\hat{p}(\cdot \mid X)$, a natural choice of non-conformity score is the negative likelihood of the output, as proposed by [Sadinle et al. \(2019\)](#):

$$S_{\text{NL}}(X_i, Y_i) = -\hat{p}(Y_i \mid X_i).$$

An important limitation of the sets defined by the score S_{NL} is that they may be empty when the predicted conditional distribution $\hat{p}(\cdot \mid X)$ is upper bounded by $-\hat{q}_\alpha$. As illustrated on [Figure 1](#), this situation typically arises when the predicted density $\hat{p}(Y \mid X)$ has a large variance. Paradoxically, in such cases, one would expect a larger prediction set to reflect the increased uncertainty—making the production of an empty or overly small set particularly problematic. As a result, even when the model accurately estimates the true conditional distribution $\mathbb{P}_{Y \mid X}$, conditional coverage may still fail to hold.

To mitigate this difficulty, [Izbicki et al. \(2022\)](#) suggest using a generalized CDF, introducing the HDP-split *conformity score*

$$S_{\text{HDP}}^-(Y \mid X) = \int_{\hat{p}(y \mid X) \leq \hat{p}(Y \mid X)} \hat{p}(y \mid X) dy = \mathbb{P}_{y \sim \hat{p}(\cdot \mid X)} (\hat{p}(y \mid X) \leq \hat{p}(Y \mid X)),$$

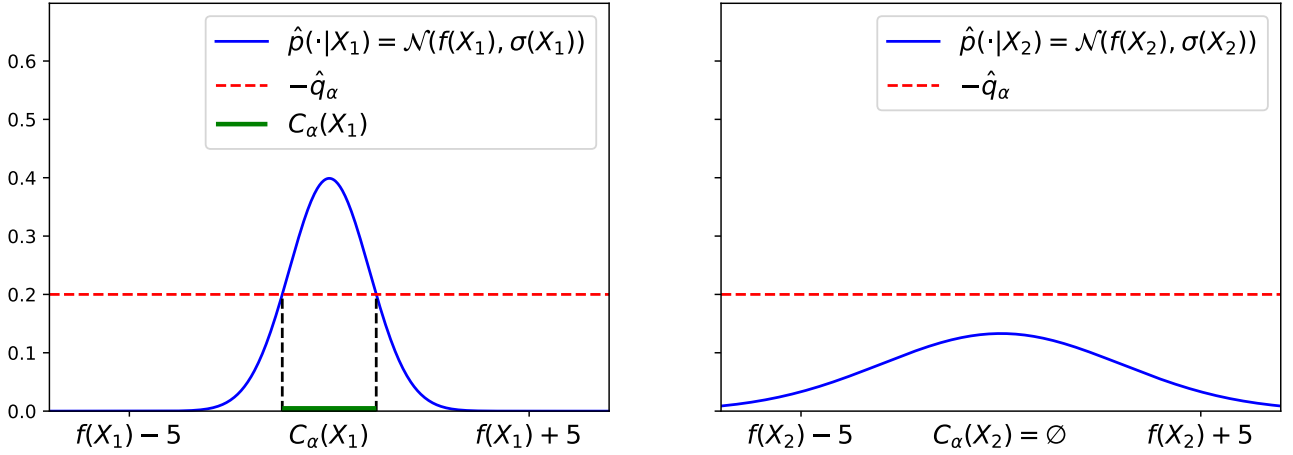


Figure 1: Illustrating a typical failure case of the S_{NL} conformal score. The $-\hat{q}_\alpha$ likelihood threshold being the same for every X , when the variance of the estimated conditional distribution $\hat{p}(\cdot|X)$ is large, the conformal set produced may be empty (right plot). This is paradoxical as a larger variance indicates more uncertainty and should translate into larger conformal sets.

yielding confidence intervals that are adaptive to the variance in $\hat{p}(\cdot|X)$. We will use this score in our work, but for consistency with the literature we will work instead with the *non-conformity score*: $S_{HDP}(X, Y) = \mathbb{P}_{y \sim \hat{p}(\cdot|X)}(\hat{p}(y|X) \geq \hat{p}(Y|X))$. The intuition is that we measure the portion $1 - \beta$ of mass of the estimated $\hat{p}(Y|X)$ in which the desired $1 - \alpha$ coverage on the calibration set is achieved. Given a new sample X the confidence interval on Y is obtained by the level set of mass $1 - \beta$ of the predicted conditional $\hat{p}(\cdot|X)$, as illustrated on Figure 2.

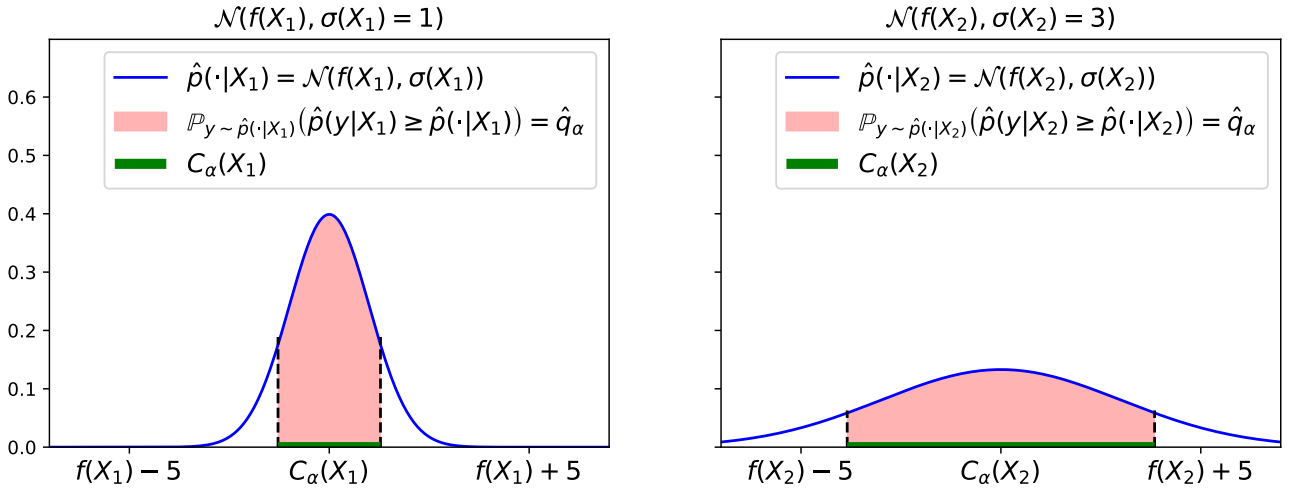


Figure 2: Illustrating the generalized CDF score S_{HDP} . With this score, a portion of the total mass of the estimated distribution $\hat{p}(\cdot|X)$ is conformalized to satisfy the required $1 - \alpha$ coverage level on the calibration set. The size of the conformal sets constructed cannot be null, as it naturally follows the variance of the estimated conditional distribution, making this score robust to the failure case exposed for S_{NL} .

Izbicki et al. (2022) demonstrate that this score guarantees asymptotic conditional coverage when \hat{p} approaches the true conditional distribution, yet for general forms of estimated conditional densities \hat{p} , the conformal scores and the resulting conformal sets are not in closed form and need to be computed by approximating high-dimensional integrals with Monte-Carlo methods.

Notation. We denote by $\mathbf{1}\{x \in A\}$ the indicator function, equal to 1 if $x \in A$ and to 0 if $x \notin A$, for some set A . We denote by S_k^{++} the space of $k \times k$ symmetric positive definite (SDP) matrices¹. We denote by δ_x the Dirac measure at point x , i.e., a probability measure that assigns mass 1 to x and 0 elsewhere. We denote $\mathcal{N}(\cdot \mid \mu, \Sigma)$ the density of a normal distribution with mean μ and covariance Σ . $[k]$ indicates the discrete set $\{1, \dots, k\}$.

2 Gaussian Conformal Prediction

2.1 Learning a Gaussian model

Let us consider the setting of multivariate regression: $\{(X_i, Y_i)\}_{i=1}^n$ are n i.i.d. feature-response pairs sampled from an unknown distribution $\mathbb{P}_{X \times Y}$ on $\mathcal{X} \times \mathcal{Y}$ where $\mathcal{Y} = \mathbb{R}^k$. Given a feature vector X , our goal is to generate a confidence set for Y using an estimate of the underlying conditional distribution $\mathbb{P}_{Y|X}$.

A natural idea is to approximate $\mathbb{P}_{Y|X}$ by a multivariate normal distribution,

$$\hat{p}(\cdot|X) = \mathcal{N}(\cdot \mid f_\theta(X), \Sigma_\phi(X)),$$

where $f_\theta : \mathbb{R}^d \rightarrow \mathbb{R}^k$ models the mean and $\Sigma_\phi : \mathbb{R}^d \rightarrow S_k^{++}$ the covariance. The underlying assumption is that our model f_θ can successfully estimate the target variable Y , up to some Gaussian noise whose covariance can depend on X .

A simple way to learn parameters θ, ϕ is to minimize the expected negative log-likelihood:

$$\mathbb{E}_{\mathbb{P}_{X \times Y}}[-\log \hat{p}(Y|X)].$$

We approximate this expectation with the empirical mean on our dataset:

$$\begin{aligned} \mathbb{E}_{\mathbb{P}_{X \times Y}}[-\log \hat{p}(Y|X)] &\approx \frac{1}{n} \sum_{i=1}^n -\log \hat{p}(Y_i|X_i) \\ &= \frac{1}{n} \sum_{i=1}^n \log((2\pi)^{k/2} \det \Sigma_\phi(X_i)^{1/2}) + \frac{1}{2} (Y_i - f_\theta(X_i))^\top \Sigma_\phi(X_i)^{-1} (Y_i - f_\theta(X_i)) \\ &= C^{ste} + \frac{1}{n} \sum_{i=1}^n -\log(\det \Sigma_\phi(X_i)^{-1/2}) + \frac{1}{2} \|\Sigma_\phi(X_i)^{-1/2} (Y_i - f_\theta(X_i))\|_2^2. \end{aligned}$$

Note that we use the parametrization $\Lambda_\phi(X) = \Sigma_\phi(X)^{-1/2}$ for the covariance matrix, which alleviates the burden of having to invert a matrix to compute the loss (cf. [Alsing et al., 2019](#)). Given that Σ_ϕ is a covariance matrix, it is SDP and thus its inverse Σ_ϕ^{-1} is also SDP. This implies that Σ_ϕ^{-1} admits a unique square-root, $\Lambda_\phi = \Sigma_\phi^{-1/2}$, that is also SDP. We can thus uniquely parametrize Λ_ϕ using its Cholesky decomposition: $\Lambda_\phi(X) = A_\phi(X)A_\phi(X)^\top$, where $A_\phi(X)$ is a lower triangular real matrix with positive diagonal entries that we learn via the parameterization ϕ . In total we need $k(k+1)/2$ learnable parameters to parameterize the multivariate normal distribution, which matches the dimension of the space S_k^{++} .

In summary, maximizing the expected likelihood is equivalent to minimizing the following loss function:

$$\mathcal{L}(f_\theta, \Lambda_\phi) = \frac{1}{n} \sum_{i=1}^n \left(-\log \det \Lambda_\phi(X_i) + \frac{1}{2} \|\Lambda_\phi(X_i)(Y_i - f_\theta(X_i))\|_2^2 \right). \quad (5)$$

¹For simplicity of notation, we assume without loss of generality that the covariance matrix is invertible. In the case of a singular covariance matrix, the density is well defined in a lower-dimensional subspace and can be written using the pseudoinverse and determinant.

We see that this Gaussian setup can be used to add uncertainty quantification on top of an existing point predictor f_θ . For f_θ fixed, \mathcal{L} can be used to learn only the covariance model Λ_ϕ .

Remark 2.1 (Jointly convex formulation). It is possible to use the parameterization $\eta_\theta(X) = -\Lambda_\phi(X)f_\theta(X)$. With this choice, the loss (5) is jointly convex in η_θ and Λ_ϕ . In practice, however, given that we parameterize these functions with neural networks, we lose the convexity anyway. We keep the current parametrization for clarity, and to retain the ability to learn only $\Lambda_\phi(X)$ on top of a fixed $f_\theta(X)$.

Remark 2.2 (Link with MSE). Our setup is closely related to learning a point-wise estimate using the mean squared error (MSE), which minimizes:

$$\text{MSE}(f_\theta) = \frac{1}{n} \sum_{i=1}^n \|Y_i - f_\theta(X_i)\|_2^2 \quad .$$

Indeed, taking $\Sigma_\phi \equiv I_k$ (so $\Lambda_\phi \equiv I_k$), minimizing the loss reduces to MSE. By allowing $\Sigma_\phi(\cdot)$ to vary, we enable the model to capture feature-dependent uncertainty while maintaining a point estimate via f_θ .

2.2 Conformalizing the Gaussian density with multivariate standardized residuals

The generalized CDF score S_{HDP} introduced by [Izbicki et al. \(2022\)](#) comes with important theoretical guarantees. However, it is generally computationally impractical, limiting its usage.

We now show that we can derive an equivalent score in closed form.² We start by rewriting this score in the particular case of a Gaussian model:

$$\begin{aligned} S_{\text{HDP}}(X, Y) &= \mathbb{P}_{y \sim \hat{p}(\cdot|X)} (\hat{p}(y|X) \geq \hat{p}(Y|X)) \\ &= \mathbb{P}_{y \sim \hat{p}(\cdot|X)} \left(\|\Sigma_\phi(X)^{-1/2}(y - f_\theta(X))\|_2^2 \leq \|\Sigma_\phi(X)^{-1/2}(Y - f_\theta(X))\|_2^2 \right) \end{aligned} \quad (6)$$

$$= \mathbb{P}_{s \sim \mathcal{N}(0, I_k)} \left(\sum_{i=1}^k s_i^2 \leq \|\Sigma_\phi(X)^{-1/2}(Y - f_\theta(X))\|_2^2 \right) \quad (7)$$

$$= F_{\chi^2(k)} \left(\|\Sigma_\phi(X)^{-1/2}(Y - f_\theta(X))\|_2^2 \right), \quad (8)$$

where (6) comes from writing the density of the two Gaussian distributions and simplifying the expressions on both sides, and (7) follows from the fact that $y \sim \hat{p}(\cdot|X) = \mathcal{N}(\cdot | f_\theta(X), \Sigma_\phi(X))$, so that the variable $\Sigma_\phi(X)^{-1/2}(y - f_\theta(X))$ is standardized and follows $\mathcal{N}(0, I_k)$. This allows us to express the probability in terms of the CDF of a χ^2 distribution with k degrees of freedom in (8).

Since $F_{\chi^2(k)}$ is strictly increasing (for any k), we can define an equivalent non-conformity score (meaning that the conformal set obtained with the two scores are the same) to S_{HDP} as:

$$S_{\text{Mah}}(X, Y) = \|\Sigma_\phi(X)^{-1/2}(Y - f_\theta(X))\|_2.$$

S_{Mah} evaluates the Mahalanobis distance induced by $\Sigma_\phi(X)$ between Y and $f_\theta(X)$. It has an intuitive interpretation as the L_2 distance between $f_\theta(X)$ and Y , reweighted by the local estimated covariance structure $\Sigma_\phi(X)$, allowing the score to take into account heteroskedasticity of the data, specifically the X -dependency of model f_θ 's uncertainty.

²Recall that we work with the *non-conformity score* induced by the HDP *conformity score*.

For a test point X_{test} , the conformal sets obtained by the Mahalanobis score are of the following form (with \hat{q}_α defined in (2)):

$$\begin{aligned} C_\alpha(X_{\text{test}}) &= \left\{ y \in \mathbb{R}^k, S_{\text{Mah}}(X_{\text{test}}, y) \leq \hat{q}_\alpha \right\} \\ &= \left\{ y \in \mathbb{R}^k, \|\Sigma_\phi(X_{\text{test}})^{-1/2}(y - f_\theta(X_{\text{test}}))\|_2 \leq \hat{q}_\alpha \right\}. \end{aligned}$$

This equation defines an ellipsoid centered in $f_\theta(X_{\text{test}})$ whose shape is parametrized by the local covariance matrix $\Sigma_\phi(X_{\text{test}})$ and whose radius is a function of the empirical quantile \hat{q}_α .

In the univariate regression setting $\mathcal{Y} = \mathbb{R}$, we recover the well-known standardized residual non-conformity score (Lei et al., 2018):

$$S_{\text{Mah}}(X, Y) = \frac{|Y - f_\theta(X)|}{\sigma_\phi(X)} =: S_{\text{Stand.}}(X, Y),$$

where $\sigma_\phi : \mathcal{X} \rightarrow \mathbb{R}_+$ is a scalar standard deviation estimate. S_{Mah} thus naturally extends standardized residuals to the multivariate setting $\mathcal{Y} \subset \mathbb{R}^k$.

Since our score S_{Mah} is equivalent to S_{HDP} , it leads to conditional coverage if $\hat{p}(y|X) dy = \mathbb{P}_{Y|X}(dy)$. However, even when this does not hold, modeling directional uncertainty through ellipsoids allows us to estimate variance along all directions efficiently, leading to predictive sets with improved conditional coverage. We demonstrate such improvements empirically in Section 6.2 and provide a theoretical justification in the following remark. Just like standardized residuals improve conditional coverage in one dimension even when the Gaussian model is not well specified, our covariance re-scaling of the residuals helps in the multivariate case.

Remark 2.3 (Mis-specified model). To achieve conditional coverage asymptotically, it is well known (see, e.g., Dheur et al. 2025) that it suffices for the conditional distribution of the score $\mathbb{P}_{S(X,Y)|X}$ to be independent of X . Let $(X, Y) \sim \mathbb{P}_{X,Y}$ with $Y \in \mathbb{R}^k$ and assume that $Y | X$ has a finite second moment almost surely. Define $f(X) = \mathbb{E}[Y | X]$ and $\Sigma(X) = \mathbb{E}[(Y - f(X))(Y - f(X))^\top | X]$, and assume that $\Sigma(X)$ is symmetric positive definite almost surely. Consider the multivariate standardized residual $U = \Sigma(X)^{-1/2}(Y - f(X))$. Then

$$\mathbb{E}[U | X] = 0 \quad \text{and} \quad \mathbb{E}[UU^\top | X] = I_k.$$

By normalizing $Y - f(X) | X$ using its second-order moment, we obtain a random variable U whose first and second conditional moments do not depend on X . Using U to define the conformal score is therefore expected to reduce its dependence on X , which in turn improves conditional coverage. However, in the non-Gaussian case, higher-order conditional moments remain uncontrolled, which prevents us from deriving more theoretical guarantees in the general setting where the distribution of $Y | X$ is unknown.

Our procedure can be compared to the framework of Johnstone and Cox (2021) who define the non-conformity score $S_{\text{ECM}}(X, Y) = \|\hat{\Sigma}^{-1/2}(Y - f_\theta(X))\|_2$, where $\hat{\Sigma}$ is the empirical covariance matrix of the entire set of training residuals $\{Z_i := Y_i - f_\theta(X_i)\}$, and thus is not feature-dependent. One way to surmount this issue, discussed by Messoudi et al. (2022), is to approximate the covariance locally by evaluating the residuals on subsets of the training data.

Recall that we obtain a closed-form expression for the non-conformity scores and the resulting confidence sets. The latter are given by thresholding at \hat{q}_α the locally induced Mahalanobis distance between the label and the estimated mean $f_\theta(X)$.

To compare these methods, Figure 3 presents a plot of the conformal sets obtained with the Mahalanobis score S_{Mah} , the negative likelihood S_{NL} , and the empirical covariance of all residuals S_{ECM} on four samples $\{X_1, X_2, X_3, X_4\}$ from a synthetic dataset. The $1 - \alpha$ marginal coverage parameter is set to 0.90. We see that the former two methods tend to produce relatively small sets when the aleatoric uncertainty is high (e.g., for X_4 , where the conditional coverage achieved by the three methods is 0.82, 0.42 and 0.32, respectively), and compensate with over-coverage when the aleatoric uncertainty is low (e.g., for X_1 , where the conditional coverage is 0.84, 0.97, 0.99, respectively).

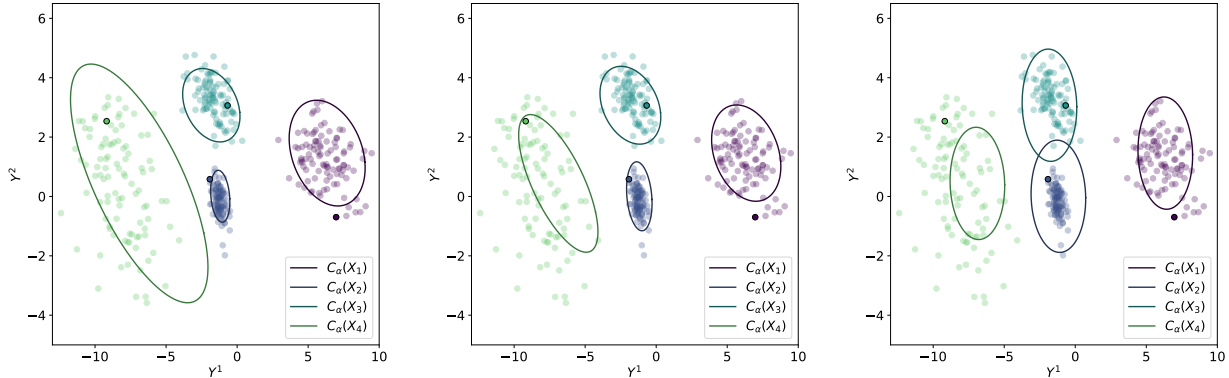


Figure 3: Conformal sets obtained with different score functions: S_{Mah} (left), S_{NL} (center) and S_{ECM} (right). Data is generated from $Y \sim f(X) + T(X)B$, where B is a standard normal vector and $T(\cdot)$ is a transformation that introduces heteroskedasticity in X (see Appendix A for details). We plot the results obtained for four different test points X_i with different colors. Dark dots show the observed label Y_i , while light dots represent additional samples from $Y | X_i$ to illustrate the shape of the conditional distribution. The ellipsoids indicate the conformal set centered in $f_\theta(X_i)$ constructed using the score used with coverage parameter $1 - \alpha$ set to 90%.

Remark 2.4 (Generalization to elliptical distributions). Our method generalizes to any elliptical distribution, and can even be extended to p -norms, that is for distributions such that there exists a non-increasing nonnegative function $g \in L^1(\mathbb{R})$ such that the density of $Y|X$ is of the form $f(y|X) = g\left(\|\Sigma_\phi(X)^{-1/2}(y - h(X))\|_p\right)$, for $h : \mathcal{X} \rightarrow \mathbb{R}^k$. Indeed, for such a distribution, the HDP-split score becomes $S_{\text{HDP}}(X, Y) = F_d\left(\|\Sigma_\phi(X)^{-1/2}(Y - f_\theta(X))\|_p\right)$ where $F_d(\cdot)$ is the potentially unknown CDF of $\|\Sigma_\phi(X)^{-1/2}(Y - f_\theta(X))\|_p$. Defining the score $S(X, Y) = \|\Sigma_\phi^{-1/2}(X)(Y - f_\theta(X))\|_p$ allows us to overcome the necessity to know the CDF of the fitted distribution in closed form. This could help fitting distributions that are less sensitive to outliers; for instance, a multivariate t-distribution (Roth, 2012).

3 Missing Outputs

In many multivariate regression problems, it is common to encounter missing values in the output vector, even at calibration time. For example, consider a climate modeling application where a system predicts multiple interdependent variables—such as temperature, humidity, and wind speed—at different geographical locations. Due to sensor malfunctions or data transmission issues, some of these target variables may be missing for certain samples. Traditional conformal prediction methods require fully observed outputs to construct valid prediction sets, which limits their applicability in such settings. We

aim to develop conformal prediction techniques that can produce reliable prediction sets, even when some components of the output vector are missing.

Method. We consider again the setting of multivariate regression: we assume that feature-response pairs (X, Y) are sampled from an unknown distribution $\mathbb{P}_{X \times Y}$ over $\mathcal{X} \times \mathcal{Y}$, where $\mathcal{Y} = \mathbb{R}^k$. Given a feature vector X , the goal is to construct a confidence set for Y using an estimate of the conditional distribution $\mathbb{P}_{Y|X}$. However, the response vector Y may not be fully observed; in particular, we assume that among its k dimensions, only a subset $\mathcal{O}_Y \subset [k]$ is revealed, and the rest are missing. This subset can vary across samples and may be random. Formally, $Y_o \in (\mathbb{R} \times \{\text{NaN}\})^k$, with NaN indicating a missing value. We distinguish Y from Y_o as we will construct valid conformal sets for Y_o , from which we will derive conformal sets for the fully observed Y .

As before, we approximate $\mathbb{P}_{Y|X}$ by a multivariate normal distribution, $\hat{p}(\cdot|X) = \mathcal{N}(\cdot|f_\theta(X), \Sigma_\phi(X))$. This enables us to define a non-conformity score in the quantile space of a χ^2 distribution, where the degrees of freedom depend on the number of observed outputs. We describe training strategies to learn the feature-dependent covariance matrix in the presence of missing outputs in Appendix B. Once the model is trained, we define the non-conformity score:

$$S_{\text{Miss}}(X, Y, \mathcal{O}_Y) = F_{\chi^2(o_Y)} \left(\left\| \Sigma_{\phi, \mathcal{O}_Y}(X)^{-1/2} (Y_{\mathcal{O}_Y} - f_{\theta, \mathcal{O}_Y}(X)) \right\|_2^2 \right),$$

where $o_Y := \text{Card}(\mathcal{O}_Y)$ denotes the number of observed components of Y , $F_{\chi^2(o_Y)}(\cdot)$ is the cumulative distribution function of a χ^2 distribution with o_Y degrees of freedom, $\Sigma_{\phi, \mathcal{O}_Y}(X)$ denotes the submatrix of $\Sigma_\phi(X)$ corresponding to the observed outputs, and similarly for $f_{\theta, \mathcal{O}_Y}(X)$ and $Y_{\mathcal{O}_Y}$ (notice that $Y_o \in (\mathbb{R} \times \{\text{NaN}\})^k$ while $Y_{\mathcal{O}_Y} \in \mathbb{R}^{o_Y}$). The intuition behind this score is the following: if $\hat{p} = \mathbb{P}_{X \times Y}$, then

$$\left\| \Sigma_{\phi, \mathcal{O}_Y}(X)^{-1/2} (Y_{\mathcal{O}_Y} - f_{\theta, \mathcal{O}_Y}(X)) \right\|_2^2 \sim \chi^2(o_Y).$$

Using the probability integral transform (David and Johnson, 1948) we obtain

$$F_{\chi^2(o_Y)} \left(\left\| \Sigma_{\phi, \mathcal{O}_Y}(X)^{-1/2} (Y_{\mathcal{O}_Y} - f_{\theta, \mathcal{O}_Y}(X)) \right\|_2^2 \right) \sim \mathcal{U}([0, 1]).$$

This transformation into the quantile space allows us to compare scores across samples, even when the number of observed outputs varies, by projecting them onto a common reference scale.³

This leads to the final prediction region for a test input X_{test} , with \hat{q}_α defined in (2):

$$C_{o, \alpha}(X_{\text{test}}) = \left\{ y_o \in (\mathbb{R} \times \{\text{NaN}\})^k \mid F_{\chi^2(o_Y)} \left(\left\| \Sigma_{\phi, \mathcal{O}_Y}(X_{\text{test}})^{-1/2} (y_o - f_{\theta, \mathcal{O}_Y}(X_{\text{test}})) \right\|_2^2 \right) \leq \hat{q}_\alpha \right\}.$$

By construction, this region satisfies the following finite-sample coverage guarantee:

$$\mathbb{P}_{X \times Y_o} (Y_{o, \text{test}} \in C_{o, \alpha}(X_{\text{test}}) \mid \{(X_i, Y_{o,i})\}_{i \in \mathcal{D}_1}) \in \left[1 - \alpha, 1 - \alpha + \frac{1}{n_2 + 1} \right).$$

Note, however, that this only guarantees coverage for the response vector with missing values Y_o . To construct a conformal set for the full vector Y , we restrict $C_{o, \alpha}(X_{\text{test}})$ to its section on the fully observed space \mathbb{R}^k ; that is, when $\mathcal{O}_Y = [k]$ we have:

$$C_{\text{full}, \alpha}(X_{\text{test}}) = \left\{ y \in \mathbb{R}^k \mid S_{\text{Miss}}(X_{\text{test}}, y, [k]) \leq \hat{q}_\alpha \right\}.$$

³Note that we focus on Gaussian models here, but it is possible to derive a non-conformity score using the HDP score on the observed outputs only, thereby extending this framework to any predictive distribution. However, doing so would suffer from the same computational issues as the classical HDP framework.

As a section of the true conformal set $C_{o,\alpha}(X_{\text{test}})$, $C_{\text{full},\alpha}(X_{\text{test}})$ has smaller coverage. While it does not ensure marginal coverage, empirical results in Section 6 suggest that the actual coverage remains close to the desired level.

Remark 3.1. Note that no assumption on the missingness mechanism is required to guarantee marginal coverage. It suffices that the missingness mechanism for the test sample coincides with that of the calibration samples, which allows us to go beyond the missing-at-random setting.

4 Partially Revealed Outputs

Consider the problem of predicting the fasting blood glucose Y^1 [g/L] and the total cholesterol Y^2 [g/L] for a patient with feature vector X . Assume that measuring these quantities induces some cost and that one can avoid performing such tests if the confidence intervals are refined enough. Consider the case where the conformal set obtained after model prediction on (Y^1, Y^2) is not refined enough and we are forced to perform a test for Y^1 . Since fasting blood glucose and total cholesterol are often correlated due to underlying physiological relationships, incorporating the information from Y^1 would allow us to refine the uncertainty quantification for Y^2 . In a classical predictive setting, integrating the revealed information would require re-training a model for Y^2 using the updated feature vector $Z = (X, Y^1)$, which is computationally expensive and often unrealistic. Instead, we propose to leverage the learned probabilistic model to adapt the sets directly without incurring any additional computation cost.

Method. Consider again a Gaussian model $\hat{p}(\cdot|X)$ that has been fit to estimate the conditional density $\mathbb{P}_{Y|X}$ using a training dataset and assume that we are given a separate calibration dataset, $\mathcal{D}_2 = \{(X_i, Y_i)\}_{i=1}^{n_2}$, of n_2 i.i.d. samples drawn from $\mathbb{P}_{X \times Y}$. Suppose that for a new test point X_{test} , we observe partial information about the output Y_{test} . Specifically, write $Y_{\text{test}} = (Y_{\text{test}}^r, Y_{\text{test}}^h)$ where Y_{test}^r is the revealed part and Y_{test}^h is the hidden (to be predicted) part. Our goal is to construct a set $C_\alpha(X_{\text{test}}, Y_{\text{test}}^r)$ such that:

$$\mathbb{P}\left(Y_{\text{test}}^h \in C_\alpha(X_{\text{test}}, Y_{\text{test}}^r)\right) = 1 - \alpha,$$

where the probability is over the randomness of the test point $(X_{\text{test}}, Y_{\text{test}})$. Leveraging information in Y_{test}^r allows us to build a prediction set that adapts to the revealed components.

A natural way to incorporate Y^r is through the conditional density $Y^h | X, Y^r$, computed as:

$$\hat{p}(Y^h|X, Y^r) = \frac{\hat{p}(Y^h, Y^r|X)}{\hat{p}(Y^r|X)} = \frac{\hat{p}(Y^h, Y^r|X)}{\int \hat{p}(Y^r, y^h|X) dy^h}.$$

For arbitrary density models $\hat{p}(\cdot|X)$, computing this conditional density introduces extra complexity due to the intractable denominator. Monte Carlo methods (Robert and Casella, 1999) can approximate the conditional, but even likelihood-based non-conformity scores become difficult to use directly without additional assumption on the fitted distribution. In our case however, since \hat{p} is Gaussian the conditional density can be computed in closed form. We denote

$$\hat{p}(\cdot|X) = \mathcal{N}\left(\cdot \mid \begin{pmatrix} f^r(X) \\ f^h(X) \end{pmatrix}, \begin{pmatrix} \Sigma^{rr}(X) & \Sigma^{rh}(X) \\ \Sigma^{hr}(X) & \Sigma^{hh}(X) \end{pmatrix}\right),$$

where the axes of revealed outputs Y^r are listed first. Conditioning on Y^r preserves Gaussianity, yielding:

$$\hat{p}(Y^h = \cdot | X, Y^r) = \mathcal{N}\left(\cdot \mid f^h(X) + \Sigma^{hr}(X)\Sigma^{rr}(X)^{-1}(Y^r - f^r(X)), \Sigma^{hh}(X) - \Sigma^{hr}(X)\Sigma^{rr}(X)^{-1}\Sigma^{rh}(X)\right).$$

Denoting

$$\begin{cases} \tilde{f}(X) & := f^h(X) + \Sigma^{hr}(X)\Sigma^{rr}(X)^{-1}(Y^r - f^r(X)) \\ \tilde{\Sigma}(X) & := \Sigma^{hh}(X) - \Sigma^{hr}(X)\Sigma^{rr}(X)^{-1}\Sigma^{rh}(X), \end{cases}$$

we can apply the same method as in Section 2.1, using the score:

$$S_{\text{Revealed}}(X, Y^r, Y^h) = \|\tilde{\Sigma}(X)^{-1/2}(Y^h - \tilde{f}(X))\|_2.$$

This yields, with the prediction set $C_\alpha(X_{\text{test}}, Y_{\text{test}}^r)$ defined in (3):

$$\mathbb{P}_{X \times Y} \left(Y_{\text{test}}^h \in C_\alpha(X_{\text{test}}, Y_{\text{test}}^r) \mid \{(X_i, Y_i)\}_{i \in \mathcal{D}_1} \right) \in \left[1 - \alpha, 1 - \alpha + \frac{1}{n_2 + 1} \right].$$

We illustrate the effectiveness of this strategy in Figure 4 with two axes (Y^1, Y^2) , when Y^1 is revealed. A naive way to infer sets for Y^2 given Y^1 would be to form the section of $C_\alpha(X_{\text{test}})$ obtained by fixing the value of Y^1 to the one revealed. We see that our updated conformal score constructs more refined confidence sets. This is confirmed by empirical results on real data in Section 6. Notice also that the baseline strategy returns empty sets for the purple dots, while our method adapts to the uncertainty in the realization of Y^1 .

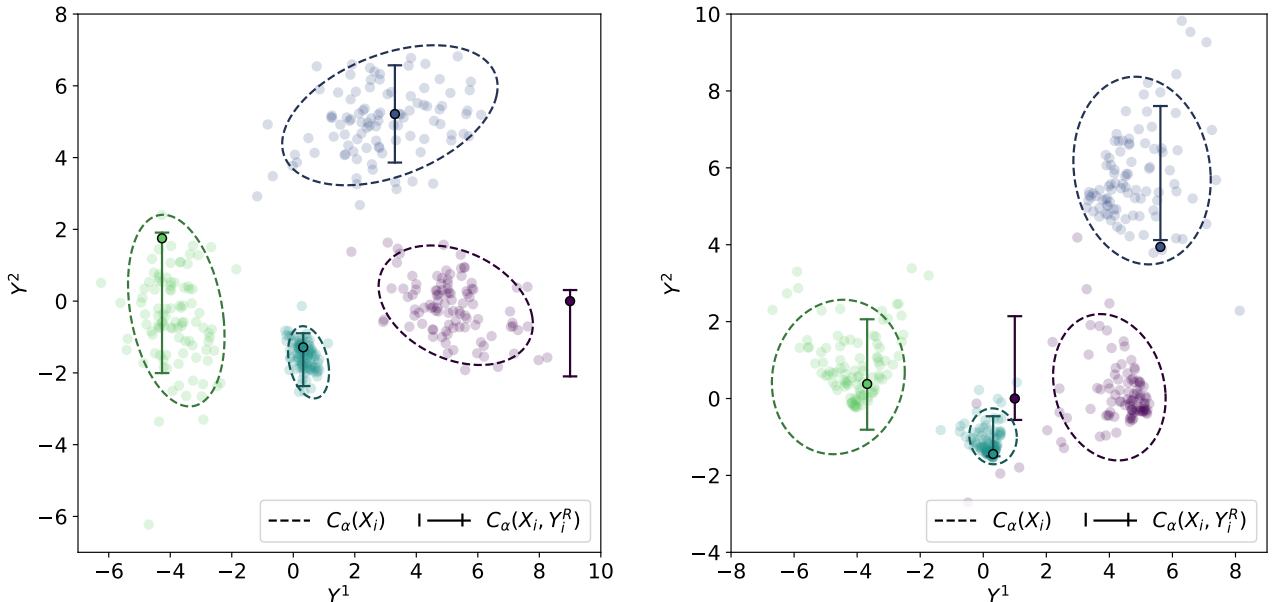


Figure 4: Conformal sets obtained for partially revealed outputs via the method described in Section 4. Data is generated from $Y \sim f(X) + T(X)B$, where B is a vector from a standard normal (left) or exponential distribution and $T(\cdot)$ is a transformation that introduces heteroskedasticity in X (see Appendix A for details). We plot the results obtained for four different test point X_i with different colors. Dark dots show the observed label Y_i , while light dots are more samples from $Y \mid X_i$ to illustrate the shape of the conditional distribution. Dashed ellipsoids represent the conformal sets constructed for the full output (Y^1, Y^2) using the Mahalanobis score with coverage parameter $1 - \alpha$ set to 90%. Full line intervals represent the confidence sets for Y^2 obtained with our updated conformal score when the value of Y^1 is revealed.

5 Projection of the Output

Consider a biomedical application where a model is trained to predict a wide array of physiological indicators—such as heart rate, oxygen saturation, blood pressure, glucose levels, and dozens of other

biomarkers, forming a high-dimensional output vector $Y \in \mathbb{R}^k$. While the model learns to predict all k variables jointly to exploit inter-dependencies and shared structure, a clinician may only be interested in a small subset of $p \ll k$ outputs relevant to a specific diagnosis or treatment—say, just glucose levels and systolic blood pressure. By propagating the uncertainty from the full model into this smaller subspace, we can construct compact and informative conformal prediction sets for the key clinical variables, maintaining statistical guarantees while focusing attention where it matters most.

Another example where these issues arise is in financial portfolio management. Suppose we have a probabilistic model that predicts the likelihood of several prices, such as the price of a non-risky asset Y^1 , gas Y^2 , and electricity Y^3 . Consider two different investment strategies whose returns can be modeled as $(R^1, R^2) := (rY^1, pY^2 + qY^3)$, with r, p, q being real-valued coefficients representing investment proportions. Directly obtaining confidence sets for the transformed variables (R^1, R^2) is beneficial because the investor’s decision-making process revolves around these quantities rather than the individual asset prices. A naive approach would be to construct separate prediction intervals for each Y^j and then propagate these intervals to R^1 and R^2 . However, such an approach fails to account for dependencies among Y^1, Y^2, Y^3 , leading to overly conservative uncertainty estimates. The goal here is to find a way to transfer the learned uncertainty over the output Y to non-conformity scores on the transformed output R . We address this by directly estimating the density of the desired transformation of the output, thereby providing more reliable confidence sets for decision making.

Method. Assume we have trained a Gaussian model $\hat{p}(\cdot|X)$ to estimate the conditional density $\mathbb{P}_{Y|X}$ using a training dataset and we are given a separate calibration dataset $\mathcal{D}_2 = \{(X_i, Y_i)\}_{i=1}^{n_2}$ of n_2 i.i.d. samples drawn from $\mathbb{P}_{X \times Y}$. Given a new feature vector X_{test} , our goal is to construct a finite-sample valid prediction set for a transformation of the output, denoted $\varphi(\cdot)$. This transformation could be, for example, a projection onto a lower-dimensional subspace, useful when Y is high-dimensional but only certain components are of interest. In general, the following inequality holds:

$$\mathbb{P}\left(Y_{\text{test}} \in \tilde{C}_\alpha(X_{\text{test}})\right) \leq \mathbb{P}\left(\varphi(Y_{\text{test}}) \in \varphi(\tilde{C}_\alpha(X_{\text{test}}))\right).$$

So when $\tilde{C}_\alpha(X_{\text{test}})$ is constructed as in (3) the sets $\varphi(\tilde{C}_\alpha(X_{\text{test}}))$ are a conservative (i.e., over-covering) prediction set for $\varphi(Y_{\text{test}})$, as we observe in Figure 5. If φ is an injection, the inequality becomes an equality, and projecting the conformal set directly preserves the exact coverage. However, when φ is not an injection, the projected set $\varphi(\tilde{C}_\alpha(X))$ may be too large.

To reduce conservativeness, we propose directly modeling the distribution of the transformed variable $\varphi(Y)$ and constructing conformal sets based on its estimated density. This allows us to build tighter sets that still guarantee exact marginal coverage.

Given our Gaussian model $\hat{p}(\cdot|X) = \mathcal{N}(\cdot|f(X), \Sigma(X))$, any linear transformation $\varphi(Y) = MY$ for M a deterministic matrix in $\mathbb{R}^{p \times k}$ preserves Gaussianity and the distribution of the transformed output is closed form:

$$\hat{p}(\varphi(Y) = \cdot|X) = \mathcal{N}(\cdot|Mf_\theta(X), M\Sigma_\phi(X)M^\top).$$

This allows us to compute level sets for $\varphi(Y)$ using the method described in Section 2, leading to the conformal score

$$S_{\text{Lin. Trans.}}(X, Y) = \|(M\Sigma_\phi(X)M^\top)^{-1/2}(MY - Mf_\theta(X))\|_2.$$

If $M\Sigma_\phi(X)M^\top$ is not full rank, the density can be defined via the disintegration theorem (see e.g., Ambrosio et al. 2005). With $C_\alpha(X_{\text{test}})$ the set defined in (3), using the score $S_{\text{Lin. Trans.}}$ we get the correct marginal coverage:

$$\mathbb{P}_{X \times Y} (MY \in C_\alpha(X) \mid \{(X_i, Y_i)\}_{i \in \mathcal{D}_1}) \in \left[1 - \alpha, 1 - \alpha + \frac{1}{n_2 + 1}\right].$$

In Figure 5, we compared the sets obtained by transforming the initial conformal sets constructed with the Mahalanobis score $\varphi(\tilde{C}_\alpha(X_{\text{test}}))$ with the set obtained by conformalizing the transformed density with $S_{\text{Lin. Trans.}}$, showing that we obtain more refined confidence sets with our method.

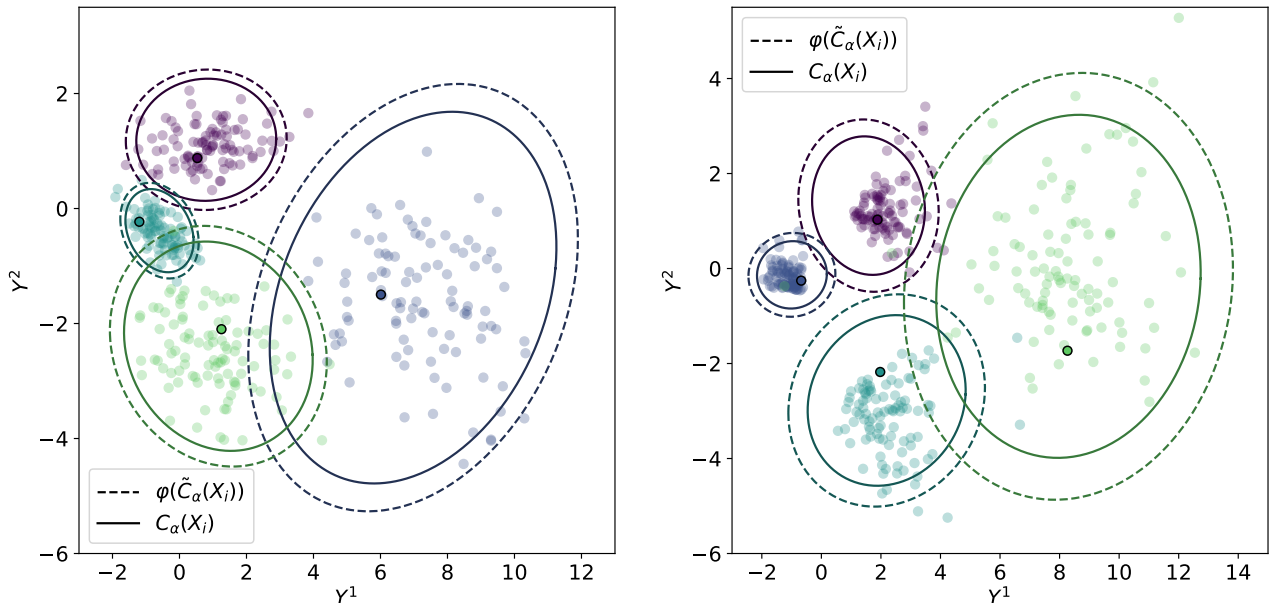


Figure 5: Comparing conformal sets obtained for projected outputs $\varphi(Y)$, by using the method presented in Section 5 (full ellipsoids), or by taking the projection $\varphi(\tilde{C}_\alpha(X_i))$ of the Mahalanobis conformal set $\tilde{C}_\alpha(X_i)$ of non-transformed outputs (dashed ellipsoids). Data is generated from $Y \sim f(X) + T(X)B$, where B is a standard normally (left) or exponentially (right) distributed vector and $T(\cdot)$ is a transformation that introduces heteroskedasticity in X (see Appendix A for details). $Y \in \mathbb{R}^3$, and we consider a projection φ of Y in \mathbb{R}^2 . The coverage parameter $1 - \alpha$ is set to 90%. We plot the results obtained for four different test point X_i with different colors. Dark dots show the observed transformed label $\varphi(Y_i)$, while light dots depict additional samples from $\varphi(Y) \mid X_i$ to illustrate the shape of the conditional distribution.

6 Experiments

The code for all our experiments is accessible on github⁴.

6.1 Baselines

We compare our results with competitive baselines that build conformal sets on top of an existing predictive model $f_\theta(\cdot)$. For all strategies, we learn $f_\theta(\cdot)$ by minimizing the mean squared error on a training dataset, then fix the model and construct confidence sets on top of its predictions. We start by describing comparative baselines.

⁴https://github.com/ElSacho/Gaussian_Conformal_Prediction

- **Empirical covariance matrix (ECM)** (Johnstone and Cox, 2021): This strategy computes the empirical covariance matrix over the residuals of the training dataset $\hat{\Sigma}$ and then uses the score $S(X, Y) = \|\hat{\Sigma}^{-1/2}(Y - f_\theta(X))\|$.
- **Optimal transport (OT)** (Thurin et al., 2025): This strategy generalizes the notion of quantiles in multivariate regression through an optimal transport map between the residuals and uniform samples over the \mathbb{R}^k unit ball.
- **MVCS** (Braun et al., 2025): This strategy generates conformal sets through a parametric function that is trained to minimize the total volume of the conformal sets obtained. Traditionally, the conformal set center $f_\theta(\cdot)$ is allowed to change to further minimize the volume of the conformal set obtained, but here we fix the center, assuming a black-box f_θ .

6.2 Synthetic datasets

In this first experiment, we focus on the empirical conditional coverage. To do so, we generate a dataset $Y \sim f(X) + T(X)B$ where $f(\cdot)$ is a deterministic function, B is a noise vector, $T(\cdot)$ introduces heteroskedasticity in the noise and $Y \in \mathbb{R}^4$. Details regarding the dataset generation are provided in Appendix A. Knowing the conditional distribution $Y|X$, we can estimate $\mathbb{P}(Y \in C_\alpha(X_i)|X_i)$, where C_α is calculated following the procedure induced by all strategies. This estimation is done by sampling $m = 1000$ points according to the known distribution $\mathbb{P}_{Y|X_i}$, and computing the coverage among those m samples.

After generating a synthetic dataset, we train f_θ and construct conformal sets ($1 - \alpha = 0.90$) for 100 randomly chosen test points X_i . For each of these, we report the conditional coverage obtained with the different methods considered in the histograms in Figure 6. We repeat this process with ten different randomly generated datasets. The noise distributions considered are Gaussian $B = \mathcal{N}(0, I_k)$ (left) and exponential $B = \mathcal{E}(\mathbf{1})$ (right). We see that the three baseline methods tend to produce over-covering conformal sets (rightmost bin) to compensate for under-covering in other regions (bins left of the 0.9 threshold). This constitutes an important failure case of conformal prediction (one that we had already observed in Figure 3), deriving from the “marginal only” guarantee that it provides. Gaussian-conformal prediction is the only method that has a distribution of conditional coverage centered around the required level $1 - \alpha$. When the conditional distribution is well estimated, results from Izbicki et al. (2022) explain this robustness, and we see that this theoretical strength translates to practice. Interestingly, we also get “almost” conditional coverage even with exponential noise, for which our Gaussian model is not well specified (right), indicating that the gains of our method are robust to complex noise scenarios.

In Table 1, we compare the average volume of the confidence sets obtained with each strategy. This table highlights one central aspect of conformal prediction: set size is not the only metric to consider when comparing different methods. Indeed, comparative baselines tend to produce smaller sets than our multivariate standardized residuals for high-variance samples. As a result, they do not produce satisfactory empirical conditional coverage, yet providing smaller sets in average. Volumes are also showed for non-heteroskedastic noise for which $T(\cdot) \equiv 1$.

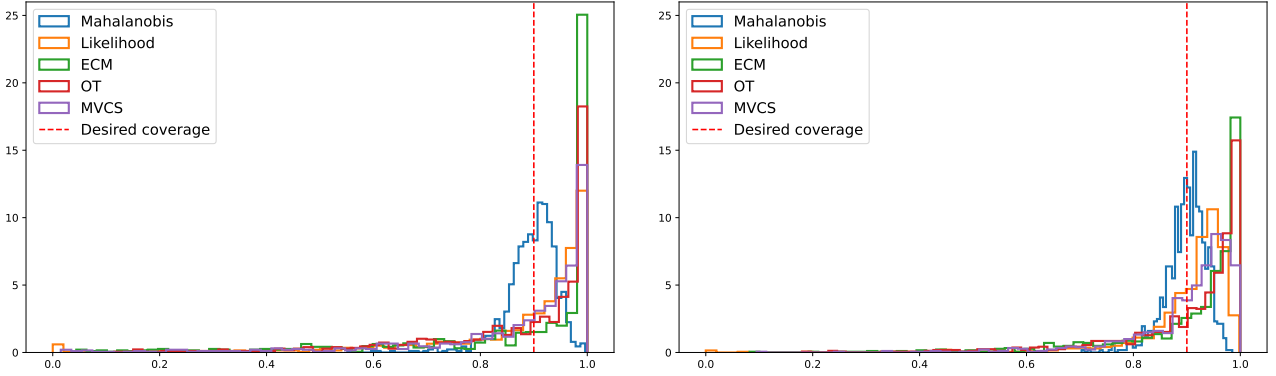


Figure 6: Histograms of conditional coverage $\mathbb{P}(Y \in C_\alpha(X_i)|X_i)$ for different test samples X_i , using different conformal prediction methods with required coverage $1 - \alpha = 0.90$ (vertical red dashed line). Aggregated results for 100 test points per dataset on ten randomly generated synthetic datasets. Heteroskedastic gaussian noise $B = \mathcal{N}(0, I_k)$ (left) and heteroskedastic exponential noise $B = \mathcal{E}(\mathbf{1})$ (right).

Noise	Mahalanobis	Likelihood	ECM	OT	MVCS
Heteroskedastic Gaussian	6.58 \pm 0.48	6.62 \pm 0.42	7.59 \pm 0.71	10.70 \pm 1.57	7.01 \pm 0.65
Heteroskedastic exponential	7.60 \pm 0.66	7.59 \pm 0.61	8.67 \pm 0.70	13.04 \pm 1.87	7.74 \pm 0.66
Fixed Gaussian	5.07 \pm 0.26	5.06 \pm 0.26	5.34 \pm 0.36	6.83 \pm 0.49	5.19 \pm 0.31
Fixed exponential	5.45 \pm 0.20	5.44 \pm 0.20	5.62 \pm 0.37	7.64 \pm 0.52	5.57 \pm 0.30

Table 1: Table for normalized volume (desired coverage 0.9) for the full vector Y with synthetic data.

6.3 Real datasets

We evaluate our approach on six datasets commonly used in multivariate regression studies (Dheur et al., 2025; Feldman et al., 2023; Wang et al., 2023; Braun et al., 2025). Details regarding the datasets and model used, including the response dimensionality, the revealed outputs and hyperparameter choices, are provided in Appendices C and D. For each dataset-method pair, we provide average volumes and marginal coverage obtained. We empathize again that set-size is not the only metric to consider when comparing conformal prediction methods and that it should be studied jointly with conditional coverage. Yet, since for real datasets the data-generating distribution is unknown, conditional coverage cannot be reliably estimated.

We set the required coverage level to $1 - \alpha = 0.90$ and provide additional results for $1 - \alpha = 0.95$ in Appendix E. Each dataset is split into four subsets—training, validation, calibration, and test—using a (70%, 10%, 10%, 10%) split.⁵ To ensure robust evaluation, results are averaged over ten independent runs, discarding the highest and lowest volume values experiments. To normalize for dimensionality, we report volumes scaled by taking their $1/k$ -th power, where k is the output dimension.

Data is pre-processed using a quantile transformation on both the features (X) and responses (Y) using `scikit-learn` (Pedregosa et al., 2011), ensuring normalization across datasets.

We report results for conformal prediction on the full output vector Y in Appendix E.

⁵Except for the energy dataset, for which the split is 55%, 15%, 15%, 15% due to the smaller amount of samples. The small number of samples does not allow to perform experiments with the OT strategy for this dataset.

6.4 Missing outputs

To experiment with missing outputs in the calibration data, we randomly add NaN values on the output vectors of the calibration dataset. The number of NaN values per output is chosen randomly between 1 and $k - 1$, with k the output dimension. We report in Tables 2 and 3 the marginal coverage achieved by the conformal sets obtained with the method described in Section 3 on a test dataset with the same missing value generating process, but also the coverage obtained for the full test vector with no missing values, for required marginal coverage $1 - \alpha = 0.90$ and $1 - \alpha = 0.95$ respectively. For the full test vector, although the conformal sets constructed do not guarantee marginal coverage, results suggests that empirical coverage remains close to the required level.

Dataset	With NaN	Full output
CASP	89.9 ± 0.5	89.1 ± 0.4
Energy	92.6 ± 3.2	86.9 ± 3.0
House	89.9 ± 0.5	85.7 ± 0.5
rf1	90.0 ± 1.2	78.7 ± 2.1
rf2	89.9 ± 0.7	82.3 ± 1.2
Taxi	89.8 ± 0.2	88.7 ± 0.5

Table 2: Marginal coverage when conformalizing with missing outputs (desired coverage 0.9).

Dataset	With NaN	Full output
CASP	94.9 ± 0.3	93.7 ± 0.4
Energy	97.3 ± 1.9	93.0 ± 1.8
House	95.0 ± 0.3	91.9 ± 0.3
rf1	95.0 ± 0.7	88.2 ± 2.0
rf2	95.0 ± 0.8	89.9 ± 1.0
Taxi	94.9 ± 0.2	93.6 ± 0.5

Table 3: Marginal coverage when conformalizing with missing outputs (desired coverage 0.95).

6.5 Partially revealed information

To experiment with the setting of partially revealed information, we reveal a portion of the test output and adjust the confidence set on the remaining dimensions. Results are displayed in Tables 4 and 5. “Bayes Mah” and “Bayes Lik.” indicate the strategy described in Section 4 based on the estimated density of $Y^h|X, Y^r$ using respectively the Mahalanobis score or the likelihood score, whereas “Sec.” indicates that we use the section on Y^r of the conformal set for the full vector Y . We see that the minimal volumes are always obtained with a method that uses the updated density $Y^h|X, Y^r$. We make the hypothesis that Bayes Lik. constructs smaller conformal sets on average (with very limited improvement though) at the expense of conditional coverage, as we observed earlier.

Dataset	Bayes Mah	Sec. Maha.	Bayes Lik.	Sec. Lik.	Sec. ECM	Sec. OT	Sec. MVCS
CASP	0.79 ± 0.06	1.15 ± 0.07	0.78 ± 0.05	1.15 ± 0.04	1.26 ± 0.02	0.94 ± 0.46	0.85 ± 0.03
Energy	0.98 ± 0.17	1.06 ± 0.23	0.89 ± 0.12	1.02 ± 0.13	1.59 ± 0.26	NA	1.11 ± 0.33
House	1.16 ± 0.07	1.32 ± 0.11	1.15 ± 0.07	1.31 ± 0.11	1.30 ± 0.07	1.51 ± 0.25	1.28 ± 0.06
rf1	0.30 ± 0.03	0.43 ± 0.05	0.31 ± 0.03	0.42 ± 0.05	0.50 ± 0.04	0.40 ± 0.02	0.38 ± 0.02
rf2	0.27 ± 0.02	0.34 ± 0.03	0.26 ± 0.02	0.33 ± 0.03	0.44 ± 0.02	0.52 ± 0.06	0.32 ± 0.02
Taxi	2.64 ± 0.02	3.10 ± 0.04	2.64 ± 0.01	3.09 ± 0.02	3.24 ± 0.03	3.12 ± 0.37	2.86 ± 0.04

Table 4: Normalized volume with partially revealed outputs (desired coverage 0.9).

Dataset	Bayes Mah	Sec. Maha.	Bayes Lik.	Sec. Lik.	Sec. ECM	Sec. OT	Sec. MVCS
CASP	89.8 ± 0.7	89.7 ± 0.5	90.0 ± 0.5	89.8 ± 0.5	90.0 ± 0.5	90.0 ± 0.8	89.6 ± 0.5
Energy	92.0 ± 1.7	91.2 ± 2.6	91.9 ± 1.6	92.3 ± 2.5	93.3 ± 2.5	NA	93.5 ± 2.9
House	90.2 ± 0.8	90.3 ± 0.9	90.3 ± 0.8	90.2 ± 0.8	89.8 ± 0.7	90.0 ± 1.1	90.5 ± 0.6
rf1	90.3 ± 1.4	89.0 ± 1.1	90.4 ± 1.5	89.2 ± 0.9	89.3 ± 1.6	89.8 ± 1.6	89.1 ± 1.6
rf2	90.5 ± 0.8	90.4 ± 0.5	90.4 ± 0.9	90.4 ± 0.9	89.1 ± 1.2	91.2 ± 1.6	90.2 ± 1.0
Taxi	90.2 ± 0.2	90.1 ± 0.4	90.1 ± 0.1	90.1 ± 0.3	90.1 ± 0.1	89.9 ± 0.6	90.1 ± 0.4

Table 5: Marginal coverage with partially revealed outputs (desired coverage 0.9).

6.6 Projection of the outputs

Here, we consider the conformal sets constructed for a low-rank linear projection of the output MY with $M \in \mathbb{R}^{p \times k}$ randomly generated. For 10 different seeds, we randomly generate the projection matrix M and evaluate the average volume and marginal coverage achieved by the strategy described in Section 5 versus projecting the sets constructed by the baselines. We report results in Tables 6 and 7. The volume of the projected MVCS set is not tractable so we don't include this baseline in the comparison.

Once again the conformal sets constructed using the projected density distribution $\hat{p}(MY|X)$ generally achieve smaller size than the projected conformal sets, with better results for the Likelihood conformal score, ostensibly at the expense of conditional coverage.

Dataset	Mahalanobis	Likelihood	ECM	OT
CASP	1.94 ± 0.59	1.93 ± 0.58	2.44 ± 0.68	2.03 ± 0.58
Energy	3.12 ± 1.53	2.71 ± 0.95	2.83 ± 1.14	NA
House	2.96 ± 0.63	2.89 ± 0.60	3.49 ± 0.69	3.01 ± 0.62
rf1	5.41 ± 11.91	1.07 ± 0.28	1.85 ± 0.37	1.11 ± 0.27
rf2	0.98 ± 0.20	0.91 ± 0.19	1.67 ± 0.33	1.39 ± 0.35
Taxi	3.87 ± 1.12	3.74 ± 1.09	4.83 ± 1.19	3.94 ± 1.00

Table 6: Normalized volume with projection of the outputs (desired coverage 0.9).

Dataset	Mahalanobis	Likelihood	ECM	OT
CASP	89.9 ± 0.4	89.9 ± 0.5	94.1 ± 0.6	90.1 ± 0.7
Energy	92.1 ± 3.8	91.5 ± 2.7	96.8 ± 1.7	NA
House	89.7 ± 0.9	89.6 ± 0.9	94.0 ± 0.5	89.7 ± 1.3
rf1	90.2 ± 1.1	90.2 ± 1.1	97.8 ± 0.5	90.2 ± 0.8
rf2	89.7 ± 1.2	89.2 ± 1.2	97.2 ± 0.5	89.7 ± 1.6
Taxi	90.1 ± 0.4	90.2 ± 0.6	95.0 ± 0.3	90.2 ± 0.5

Table 7: Marginal coverage with projection of the outputs (desired coverage 0.9).

7 Conclusions

In this paper, we introduced *Gaussian-conformal prediction*, a framework that combines the strengths of density-based conformal prediction with the flexibility of Gaussian models. The result is a natural generalization of the popular one-dimensional standardized residuals to the multivariate regression setting. Our method inherits the additional theoretical guarantees of general density-based methods, highlighted by [Izbicki et al. \(2022\)](#), while being the first method of this kind for which the scores and resulting conformal sets can be computed in closed form. We highlight in our empirical work that these guarantees translate into approximate conditional coverage in practice, which constitutes an encouraging step towards this overarching goal. By learning a parametric uncertainty model, Gaussian-conformal prediction can be applied post-hoc, on top of an existing predictor, making it especially suited for practical deployment. Finally, the flexibility of Gaussian models allows for several extensions of traditional conformal prediction. Gaussian-conformal prediction handles missing values in the output vectors, refines conformal sets when the output is partially revealed and provides valid conformal set for low-rank transformations of the outputs.

It remains difficult, however, to assess conditional coverage on real-world datasets, which limits our empirical evaluation to synthetic datasets. Furthermore, our method requires learning a full covariance matrix, which can be challenging at scale.

Acknowledgements

Authors acknowledge funding from the European Union (ERC-2022-SYG-OCEAN-101071601). Views and opinions expressed are however those of the author(s) only and do not necessarily reflect those of the European Union or the European Research Council Executive Agency. Neither the European Union nor the granting authority can be held responsible for them. This publication is part of the Chair «Markets and Learning», supported by Air Liquide, BNP PARIBAS ASSET MANAGEMENT Europe, EDF, Orange and SNCF, sponsors of the Inria Foundation. This work has also received support from the French government, managed by the National Research Agency, under the France 2030 program with the reference «PR[AI]RIE-PSAI» (ANR-23-IACL-0008).

References

Alsing, J., T. Charnock, S. Feeney, and B. Wandelt (2019). Fast likelihood-free cosmology with neural density estimators and active learning. *Monthly Notices of the Royal Astronomical Society* 488(3),

4440–4458.

- Ambrosio, L., N. Gigli, and G. Savaré (2005). *Gradient Flows: in Metric Spaces and in the Space of Probability Measures*. Springer.
- Angelopoulos, A. N. and S. Bates (2023). Conformal prediction: A gentle introduction. *Foundations and Trends in Machine Learning* 16(4), 494–591.
- Braun, S., L. Aolaritei, M. I. Jordan, and F. Bach (2025). Minimum volume conformal sets for multivariate regression. *arXiv preprint arXiv:2503.19068*.
- David, F. and N. Johnson (1948). The probability integral transformation when parameters are estimated from the sample. *Biometrika* 35(1/2), 182–190.
- Dheur, V., M. Fontana, Y. Estievenart, N. Desobry, and S. B. Taieb (2025). Multi-output conformal regression: A unified comparative study with new conformity scores. *International Conference on Machine Learning*.
- English, E. and C. Lippert (2025). Japan: Joint adaptive prediction areas with normalising-flows. *arXiv preprint arXiv:2505.23196*.
- Feldman, S., S. Bates, and Y. Romano (2023). Calibrated multiple-output quantile regression with representation learning. *Journal of Machine Learning Research* 24(24), 1–48.
- Feldman, S., S. Bates, and Y. Romano (2025). Conformal prediction with corrupted labels: Uncertain imputation and robust re-weighting. *arXiv preprint arXiv:2505.04733*.
- Foygel Barber, R., E. J. Candès, A. Ramdas, and R. J. Tibshirani (2021). The limits of distribution-free conditional predictive inference. *Information and Inference: A Journal of the IMA* 10(2), 455–482.
- Izbicki, R., G. Shimizu, and R. B. Stern (2022). CD-split and HPD-split: Efficient conformal regions in high dimensions. *Journal of Machine Learning Research* 23(87), 1–32.
- Johnstone, C. and B. Cox (2021). Conformal uncertainty sets for robust optimization. In *Conformal and Probabilistic Prediction and Applications*, Volume 152, pp. 72–90.
- Klein, M., L. Bethune, E. Ndiaye, and M. Cuturi (2025). Multivariate conformal prediction using optimal transport. *arXiv preprint arXiv:2502.03609*.
- Kong, J., Y. Liu, and G. Yang (2025). Fair conformal prediction for incomplete covariate data. *arXiv preprint arXiv:2504.12582*.
- Le Morvan, M., J. Josse, E. Scornet, and G. Varoquaux (2021). What’s a good imputation to predict with missing values? In *Advances in Neural Information Processing Systems*, pp. 11530–11540.
- Lei, J., M. G’Sell, A. Rinaldo, R. J. Tibshirani, and L. Wasserman (2018). Distribution-free predictive inference for regression. *Journal of the American Statistical Association* 113(523), 1094–1111.
- Lei, J. and L. Wasserman (2014). Distribution-free prediction bands for non-parametric regression. *Journal of the Royal Statistical Society Series B: Statistical Methodology* 76(1), 71–96.

- Messoudi, S., S. Destercke, and S. Rousseau (2022). Ellipsoidal conformal inference for multi-target regression. In *Conformal and Probabilistic Prediction with Applications*, Volume 179, pp. 294–306.
- Neeven, J. and E. Smirnov (2018, 11–13 Jun). Conformal stacked weather forecasting. In *Conformal and Probabilistic Prediction and Applications*, Volume 91, pp. 220–233.
- Papadopoulos, H., K. Proedrou, V. Vovk, and A. Gammerman (2002). Inductive confidence machines for regression. In *European conference on machine learning*, pp. 345–356.
- Pedregosa, F., G. Varoquaux, A. Gramfort, V. Michel, B. Thirion, O. Grisel, M. Blondel, P. Prettenhofer, R. Weiss, V. Dubourg, et al. (2011). Scikit-learn: Machine learning in Python. *Journal of Machine Learning Research* 12, 2825–2830.
- Plassier, V., A. Fishkov, M. Guizani, M. Panov, and E. Moulines (2025). Probabilistic conformal prediction with approximate conditional validity. *International Conference on Learning Representations*.
- Principato, G., G. Stoltz, Y. Amara-Ouali, Y. Goude, B. Hamrouche, and J.-M. Poggi (2024). Conformal prediction for hierarchical data. *arXiv preprint arXiv:2411.13479*.
- Robert, C. P. and G. Casella (1999). *Monte Carlo Statistical Methods*. Springer.
- Romano, Y., E. Patterson, and E. Candès (2019). Conformalized quantile regression. *Advances in Neural Information Processing systems* 32.
- Roth, M. (2012). *On the Multivariate t Distribution*. Linköping University Electronic Press.
- Sadinle, M., J. Lei, and L. Wasserman (2019). Least ambiguous set-valued classifiers with bounded error levels. *Journal of the American Statistical Association* 114 (525), 223–234.
- Sampson, M. and K.-S. Chan (2024). Flexible conformal highest predictive conditional density sets. *arXiv preprint arXiv:2406.18052*.
- Shafer, G. and V. Vovk (2008). A tutorial on conformal prediction. *Journal of Machine Learning Research* 9(3), 371–421.
- Thurin, G., K. Nadjahi, and C. Boyer (2025). Optimal transport-based conformal prediction. *International Conference on Machine Learning*.
- Tumu, R., M. Cleaveland, R. Mangharam, G. Pappas, and L. Lindemann (2024). Multi-modal conformal prediction regions by optimizing convex shape templates. In *6th Annual Learning for Dynamics & Control Conference*, pp. 1343–1356.
- Vovk, V. (2012). Conditional validity of inductive conformal predictors. In *Asian Conference on Machine Learning*, pp. 475–490.
- Vovk, V., A. Gammerman, and G. Shafer (2005). *Algorithmic Learning in a Random World*. Springer.
- Wang, Z., R. Gao, M. Yin, M. Zhou, and D. Blei (2023). Probabilistic conformal prediction using conditional random samples. In *International Conference on Artificial Intelligence and Statistics*, Volume 206, pp. 8814–8836.

Wieslander, H., P. J. Harrison, G. Skogberg, S. Jackson, M. Fridén, J. Karlsson, O. Spjuth, and C. Wählby (2020). Deep learning with conformal prediction for hierarchical analysis of large-scale whole-slide tissue images. *IEEE Journal of Biomedical and Health Informatics* 25(2), 371–380.

Zaffran, M., A. Dieuleveut, J. Josse, and Y. Romano (2023). Conformal prediction with missing values. In *International Conference on Machine Learning*, Volume 202, pp. 40578–40604.

Zaffran, M., J. Josse, Y. Romano, and A. Dieuleveut (2024). Predictive uncertainty quantification with missing covariates. *arXiv preprint arXiv:2405.15641*.

Zhou, X., B. Chen, Y. Gui, and L. Cheng (2025). Conformal prediction: A data perspective. *ACM Computing Surveys*.

Appendix

A Synthetic dataset generation

We generate data similarly to [Braun et al. \(2025\)](#), and recall their model here. The model is $Y \sim f(X) + T(X)B$, where $X \sim \mathcal{N}(0, I_d)$ and $Y \in \mathbb{R}^k$. The noise term B follows a fixed distribution and is modulated by the transformation $T(X)$. The transformation function $T(X)$ is defined as

$$T(X) = r(X) \exp \left(\sum_{i=1}^K w_i(X) \log R_i \right), \quad (9)$$

where $r(X)$ scales the transformation, and the summation interpolates between K randomly generated fixed rotation matrices R_i in the Lie algebra via the log-Euclidean framework, ensuring valid rotations.

The interpolation weights $w_i(X)$ are determined based on the proximity of X to K anchor points in \mathbb{R}^d , following an inverse squared distance scheme:

$$\tilde{w}_i(X) = \frac{1}{\|X - X_i\|^4}, \quad w_i(X) = \frac{\tilde{w}_i(X)}{\sum_j \tilde{w}_j(X)}.$$

This formulation allows the covariance of $Y|X$ to vary smoothly with X , generating complex, structured heteroskedastic noise patterns.

The radius function is set to $r(X) = \|X\|/2 + X^\top v + 0.15$, and the function $f(X)$ is defined as

$$f(X) = 2(\sin(X^\top \beta) + \tanh((X \odot X)^\top \beta) + X^\top J_2),$$

where v and β are random fixed parameters in $\mathbb{R}^{d \times k}$, and J_2 is a coefficient matrix with all entries set to zero except for $(1, 1)$ and $(2, 2)$, which are set to 1.

We generate a dataset of 30,000 samples from this distribution, which is then split into training, validation, calibration, and test sets.

B Learning a feature-dependent covariance matrix in the presence of missing outputs

Data imputation. This strategy imputes missing outputs by chosen values. The loss (5) is therefore unchanged. The missing outputs can either be replaced by their correspond predictive values in the vector $f_\theta(X)$, or by an average of all outputs, or more advanced strategies. We refer to [Le Morvan et al. \(2021\)](#) for a more detailed overview of data imputation.

Adapting the cross entropy. Let $o_Y := \text{Card}(\mathcal{O}_Y)$ denote the number of observed components of Y . Let $\Sigma_{\phi, \mathcal{O}_Y}(X)$ denote the submatrix of $\Sigma_{\phi}(X)$ corresponding to the observed outputs, and similarly for $f_{\theta, \mathcal{O}_Y}(X)$. Define the conditional density over the observed outputs as

$$\hat{p}_{\mathcal{O}_Y}(\cdot|X, \mathcal{O}_Y) = \mathcal{N}(\cdot|f_{\theta, \mathcal{O}_Y}(X), \Sigma_{\phi, \mathcal{O}_Y}(X)).$$

We can fit $\hat{p}_{\mathcal{O}_Y}$ by minimizing the negative log-likelihood:

$$\mathbb{E}_{\mathbb{P}_{X \times Y_o}}[-\log \hat{p}_{\mathcal{O}_Y}(Y_o|X)],$$

which we approximate using the empirical average over the dataset:

$$\begin{aligned} \mathbb{E}_{\mathbb{P}_{X \times Y}}[-\log \hat{p}_{\mathcal{O}_Y}(Y_{\mathcal{O}_Y}|X)] &\simeq \frac{1}{n} \sum_{i=1}^n \left[-\log \left(\det \Sigma_{\phi, \mathcal{O}_{Y_i}}(X_i)^{-1/2} \right) + \frac{1}{2} \left\| \Sigma_{\phi, \mathcal{O}_{Y_i}}(X_i)^{-1/2} (Y_i - f_{\theta, \mathcal{O}_{Y_i}}(X_i)) \right\|_2^2 \right] \\ &\quad + C^{\text{ste}}(Y_i). \end{aligned}$$

Compared to (5), we cannot express this objective in terms of a matrix $\Lambda_{\phi, \mathcal{O}_Y}$, because we are not extracting the submatrix from Λ_{ϕ} , but rather computing the inverse of a submatrix of Σ_{ϕ} . This makes training more computationally expensive, as it requires a matrix inversion at each iteration.

C Details on the dataset

See Table 8. For the experimental setup with missing values and projection of the outputs, we added one feature in the output vector when the dimension of the output is two.

Dataset	Number of samples	Dimension of feature	Dimension of response	Number of revealed outputs
CASP	45730	8	2	1
Energy	768	8	2	1
House	21613	17	2	1
rf1	9125	64	8	5
rf2	9125	576	8	5
Taxi	61286	6	2	1

Table 8: Description of the datasets.

D Hyperparameters

Each dataset requires its own hyperparameter tuning. In Table 9, we show the hyperparameters used for the CASP dataset. Full details for all experiments can be found in our GitHub repository.

E Additional results

E.1 Full vector

In Tables 10, 11, 12 and 13 we report the average normalized volume and marginal coverage obtained on the different datasets considered with our method and baselines for the full output vector Y with required marginal coverage $1 - \alpha = 0.90$ and 0.95 .

Hyperparameter	Value
Hidden dimension (center)	256
Number of hidden layers (center)	1
Activation function (center)	ReLU
Hidden dimension (matrix)	256
Number of hidden layers (matrix)	0
Activation function (matrix)	ReLU
Optimizer	Adam
Number of epochs	250
Batch size	100
Learning rate (model)	0.0001
Learning rate (matrix)	0.005
Learning scheduler	CosineAnnealingLR

Table 9: Hyper-parameters on the CASP dataset.

Dataset	Mahalanobis	Likelihood	ECM	OT	MVCS
CASP	1.43 ± 0.05	1.43 ± 0.03	1.52 ± 0.02	1.45 ± 0.04	1.30 ± 0.04
Energy	1.23 ± 0.22	1.16 ± 0.09	1.64 ± 0.22	NA	1.27 ± 0.30
House	1.44 ± 0.07	1.42 ± 0.06	1.44 ± 0.04	1.44 ± 0.05	1.37 ± 0.05
rf1	0.41 ± 0.04	0.40 ± 0.04	0.42 ± 0.01	0.44 ± 0.03	0.37 ± 0.02
rf2	0.34 ± 0.02	0.33 ± 0.02	0.41 ± 0.01	0.52 ± 0.04	0.32 ± 0.02
Taxi	3.34 ± 0.04	3.34 ± 0.03	3.44 ± 0.02	3.33 ± 0.06	3.25 ± 0.02

Table 10: Normalized volume (desired coverage 0.9) for the full vector Y .

Dataset	Mahalanobis	Likelihood	ECM	OT	MVCS
CASP	89.7 ± 0.5	89.8 ± 0.5	90.0 ± 0.5	90.0 ± 0.8	89.6 ± 0.5
Energy	91.2 ± 2.6	92.3 ± 2.5	93.3 ± 2.5	NA	93.5 ± 2.9
House	90.3 ± 0.9	90.2 ± 0.8	89.8 ± 0.7	90.0 ± 1.1	90.5 ± 0.6
rf1	89.0 ± 1.1	89.2 ± 0.9	89.3 ± 1.6	89.8 ± 1.6	89.1 ± 1.6
rf2	90.4 ± 0.5	90.4 ± 0.9	89.1 ± 1.2	91.2 ± 1.6	90.2 ± 1.0
Taxi	90.1 ± 0.4	90.1 ± 0.3	90.1 ± 0.1	89.9 ± 0.6	90.1 ± 0.4

Table 11: Marginal coverage for the full vector Y (desired coverage 0.9).

E.2 Partially revealed outputs

In Tables 14 and 15, we report the average normalized volume and marginal coverage obtained on the different datasets considered with our method and baselines when some dimensions of the output vector Y are revealed and the conformal sets are refined for the unobserved dimensions only. Required marginal coverage is set to $1 - \alpha = 0.95$.

Bayes Mah & Bayes Lik. indicate the strategy described in Section 4 using the estimated density of $Y^h|X, Y^r$ using respectively the Mahalanobis score or the likelihood score, whereas ‘‘Sec.’’ indicates that we use the section on Y^r of the conformal set for the full vector Y .

Dataset	Mahalanobis	Likelihood	ECM	OT	MVCS
CASP	1.82 ± 0.09	1.80 ± 0.06	1.94 ± 0.03	2.15 ± 0.11	28.78 ± 46.34
Energy	1.77 ± 0.54	1.71 ± 0.46	2.16 ± 0.36	NA	1.46 ± 0.22
House	1.95 ± 0.11	1.91 ± 0.11	1.86 ± 0.05	2.05 ± 0.15	1.79 ± 0.07
rf1	0.53 ± 0.05	0.70 ± 0.54	0.57 ± 0.02	0.48 ± 0.02	0.46 ± 0.02
rf2	0.42 ± 0.03	0.41 ± 0.02	0.55 ± 0.02	0.59 ± 0.04	0.45 ± 0.04
Taxi	4.09 ± 0.04	4.08 ± 0.04	4.17 ± 0.04	3.94 ± 0.03	3.97 ± 0.05

Table 12: Table for normalized volume (desired coverage 0.95) for the full vector Y .

Dataset	Mahalanobis	Likelihood	ECM	OT	MVCS
CASP	94.8 ± 0.3	94.8 ± 0.4	95.0 ± 0.4	95.1 ± 0.3	94.9 ± 0.2
Energy	97.8 ± 1.3	97.4 ± 1.6	97.4 ± 2.1	NA	97.8 ± 0.9
House	95.0 ± 0.5	94.9 ± 0.5	94.7 ± 0.7	95.4 ± 0.5	95.1 ± 0.4
rf1	95.2 ± 0.9	95.2 ± 0.9	94.5 ± 0.7	96.2 ± 0.9	94.8 ± 0.8
rf2	95.2 ± 0.4	94.9 ± 0.6	94.9 ± 0.6	95.7 ± 0.7	94.9 ± 0.7
Taxi	95.2 ± 0.4	95.3 ± 0.3	95.0 ± 0.1	95.0 ± 0.2	95.1 ± 0.4

Table 13: Table for coverage for the full vector Y (desired coverage 0.95).

Dataset	Bayes Mah	Sec. Maha.	Bayes Lik.	Sec. Lik.	Sec. ECM	Sec. OT	Sec. MVCS
CASP	1.12 ± 0.08	1.56 ± 0.11	1.09 ± 0.06	1.53 ± 0.07	1.69 ± 0.04	1.93 ± 0.92	5.26 ± 7.05
Energy	1.48 ± 0.48	1.61 ± 0.49	1.40 ± 0.43	1.58 ± 0.43	2.16 ± 0.39	NA	1.38 ± 0.23
House	1.66 ± 0.11	1.85 ± 0.11	1.65 ± 0.10	1.82 ± 0.11	1.75 ± 0.09	2.47 ± 0.45	1.77 ± 0.06
rf1	0.40 ± 0.04	0.59 ± 0.08	0.46 ± 0.12	0.75 ± 0.55	0.72 ± 0.06	0.45 ± 0.03	0.52 ± 0.04
rf2	0.36 ± 0.03	0.46 ± 0.04	0.34 ± 0.03	0.45 ± 0.03	0.64 ± 0.03	0.64 ± 0.11	0.49 ± 0.04
Taxi	3.38 ± 0.01	3.98 ± 0.02	3.40 ± 0.02	3.97 ± 0.03	4.12 ± 0.06	4.10 ± 0.46	3.79 ± 0.06

Table 14: Table for normalized volume with partially revealed outputs (desired coverage 0.95).

Dataset	Bayes Mah	Sec. Maha.	Bayes Lik.	Sec. Lik.	Sec. ECM	Sec. OT	Sec. MVCS
CASP	94.8 ± 0.5	94.8 ± 0.3	94.8 ± 0.4	94.8 ± 0.4	95.0 ± 0.4	95.1 ± 0.3	94.9 ± 0.2
Energy	97.5 ± 1.5	97.8 ± 1.3	97.5 ± 1.3	97.4 ± 1.6	97.4 ± 2.1	NA	97.8 ± 0.9
House	95.0 ± 0.5	95.0 ± 0.5	95.0 ± 0.5	94.9 ± 0.5	94.7 ± 0.7	95.4 ± 0.5	95.1 ± 0.4
rf1	95.2 ± 0.7	95.2 ± 0.9	95.0 ± 0.6	95.2 ± 0.9	94.5 ± 0.7	96.2 ± 0.9	94.8 ± 0.8
rf2	95.5 ± 0.6	95.2 ± 0.4	95.4 ± 0.6	94.9 ± 0.6	94.9 ± 0.6	95.7 ± 0.7	94.9 ± 0.7
Taxi	95.0 ± 0.2	95.2 ± 0.4	95.1 ± 0.2	95.3 ± 0.3	95.0 ± 0.1	95.0 ± 0.2	95.1 ± 0.4

Table 15: Table for coverage with partially revealed outputs (desired coverage 0.95).

E.3 Projection of the outputs

In Tables 16 and 17, we report the average normalized volume and marginal coverage obtained on the different datasets considered with our method and baselines for conformal sets constructed to contain

the transformed output $\varphi(Y)$ with required marginal coverage $1 - \alpha = 0.95$. The volume of the projected MVCS set is not tractable so we don't include this baseline in the comparison.

Dataset	Mahalanobis	Likelihood	ECM	OT
CASP	2.38 ± 0.68	2.35 ± 0.67	2.98 ± 0.79	2.76 ± 0.77
Energy	3.77 ± 1.63	3.53 ± 1.27	3.65 ± 1.53	NA
House	3.86 ± 0.92	3.79 ± 0.85	4.28 ± 0.84	4.11 ± 0.69
rf1	7.14 ± 15.73	1.48 ± 0.41	2.47 ± 0.48	1.45 ± 0.30
rf2	1.29 ± 0.28	1.21 ± 0.26	2.39 ± 0.56	2.09 ± 0.65
Taxi	4.69 ± 1.35	4.54 ± 1.32	5.90 ± 1.43	4.68 ± 1.10

Table 16: Table for normalized volume with projection of the outputs (desired coverage 0.95).

Dataset	Mahalanobis	Likelihood	ECM	OT
CASP	94.9 ± 0.3	95.0 ± 0.3	97.1 ± 0.3	94.8 ± 0.8
Energy	97.0 ± 2.0	97.1 ± 1.7	98.8 ± 1.2	NA
House	94.6 ± 1.1	94.6 ± 1.0	97.0 ± 0.2	95.4 ± 0.7
rf1	94.9 ± 0.8	94.9 ± 0.9	98.8 ± 0.3	95.5 ± 0.7
rf2	94.9 ± 0.8	94.9 ± 0.8	98.7 ± 0.3	95.5 ± 1.2
Taxi	95.1 ± 0.2	95.1 ± 0.3	97.5 ± 0.3	94.9 ± 0.4

Table 17: Table for coverage with projection of the outputs (desired coverage 0.95).